Rijksdienst voor Ondernemend Nederland

Openbaar eindrapport FlamingoPV

Gegevens project

- Projectnummer: TEUE118011
- Projecttitel: FlamingoPV
- Penvoerder en medeaanvragers: HyET Solar B.V., Technische Universiteit Delft
- Projectperiode: March 2019 – September 2022
- Publicatiedatum openbaar rapport: 23 February 2023

Samenvatting van uitgangspunten, doelstelling en samenwerkende partijen

Background: Thin-film silicon, flexible solar modules have a high potential for large-scale deployment to accelerate the energy transition. Given their lightweight and low balance of system costs, these modules can be used in many applications in which weight is a very important requirement (ships, building-integrated photovoltaics, large-scale utilities). Therefore, it is instrumental to develop high-efficiency thin-film silicon solar modules to accelerate this deployment. Currently, the efficiency in the hydrogenated amorphous silicon (a-Si:H) single junction configuration, is around 7% before light-induced degradation. In order to increase efficiency, a tandem hydrogenated amorphous/nanocrystalline silicon (a-Si:H/nc-Si:H) configuration (also known as micromorph) has to be deployed, so the sunlight spectrum is utilized better. In order to increase the tandem efficiency from 10 to 12%, some aspects need to be optimized, such as i) substrate texturing to enhance scattering of NIR light in the bottom cell, ii) development of a back reflector that best redirects light in the bottom cell, and iii) development of high V_{OC} absorber layers (employing hydrogen profiling, especially for the bottom cell).

Objectives: The objectives of this project are to develop all the building blocks for the demonstration of a high-efficiency tandem module. Therefore, a proper pre-treatment of the aluminum foil, on top of which the silicon layer stack is deposited, has to be developed for the tandem application. More precisely put, the surface should be able to scatter light beyond 800 nm in order to facilitate light absorption in the bottom cell [1][2]. Incidentally, such a surface also facilitates the growth of high-quality nc-Si:H [3]. The objective of this project is to transfer knowledge regarding scientific aspects of Al processing from lab-scale to fab-scale at HyET Solar.

Collaborating parties: Delft University of Technology, HyET Solar Netherlands B.V.

Beschrijving van de behaalde resultaten, de knelpunten en het perspectief voor toepassing

0. HyET Solar Powerfoil: roll-to-roll process flow and building blocks needed to reaching high efficiency

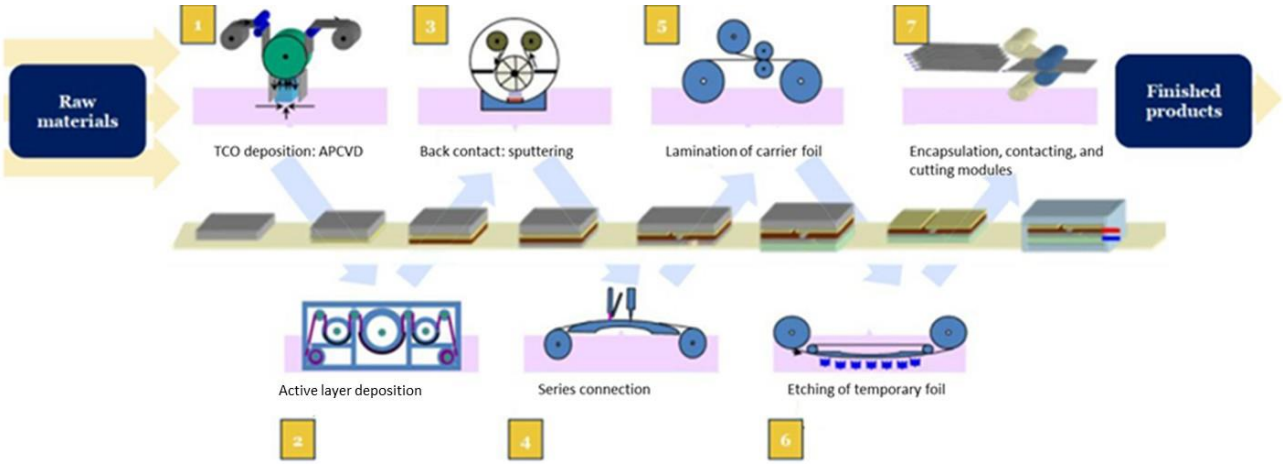

Figure 0.1. HyET Solar Powerfoil PV module process flow.

HyET Solar has set the new standard in flexible thin-film PV solar energy for the industry with its Powerfoil and it is the ambition to manufacture Powerfoil with an efficiency of 12%. Powerfoil is a thin film silicon (TF-Si) based module that is not deposited on glass but on commodity-based polymers. This results in unique characteristics such as flexibility, drastically reduced weight, strongly reduced raw material needs, and lower production and installation costs while ensuring robustness and longevity. The production itself makes use of abundant and non-toxic materials (e.g., silicon, aluminum, and polymers), while avoiding using scarce and/or toxic materials such as cadmium, indium, gallium, nickel, arsenic or tellurium. A schematic overview of the roll-to-roll process flow is shown in Figure 0.1.

The TF-Si PV active layer of Powerfoil is only two to four micrometers thin – compared to about 150-200 micrometers of a typical c-Si wafer. 99% of the Powerfoil module is made of different polymer encapsulation materials on opposite sides of the PV active materials in the module, protecting the active layer against weather influences and physical contact/scratches. The layer structure is used to scatter the incoming light optimally. The multiple layers increase the optical path, while the electric path is kept as short as needed.

Several components in the Powerfoil product are of key importance to boost performance and reliability to high levels. To this end, such building blocks that are needed to reach the desired efficiency have been analyzed and developed in collaboration with TU Delft and this report outlines the progress on those topics. This includes the texturing of the Al foil that is used as a temporary carrier for the thin film layer stack in the manufacturing process, the removal of precipitants from the Al foil, improving the quality of the module interconnect, other steps needed to reach the goal of 12% stable product, and finally a lifecycle analysis. Results on these topics are discussed in this order in the subsequent sections.

1. Texturing of the Al foil

a. Introduction

In this section, we analyze the pre-treatment of the Al temporary substrate to introduce surface texture in the Al foil. This is instrumental to improve light scattering at long wavelength (800 – 1100 nm) and also to facilitate high quality nc-Si:H growth for the bottom/middle cell in tandem/triple junction solar cells [4]. Therefore, it is very important to pre-treat the temporary Al substrate in order to have the right structural properties to reach the aforementioned objectives. The metrics used to characterize the surface morphology are measured either with AFM or confocal microscopy. In the first case, the 2D auto-correlation length (L_C) and root-mean-square roughness (σ_{rms}) are used. These parameters correspond physically to the average width and depth of the structures on the substrate. The ratio σ_{rms}/L_C is commonly known as the aspect ratio. It is well known that the aspect ratio of the substrate should be > 10% to be able to grow high quality nc-Si:H [5]. In the case of confocal microscopy measurements, the arithmetic mean peak curvature (S_{PC}) is used as a metric.

b. Baseline texturing characterization

The very first approach to this problem is to characterize the factory baseline. This is the standard pre-treatment of the Al foil operated at HyET Solar in the factory. The pre-treatment (alternatively, we use the term 'texturing' interchangeably) is conducted using sodium hydroxide diluted in water (0.1M) at 35 °C with a certain web-speed. In figure 1.1, SEM and AFM measurements of such textured Al foil are shown.

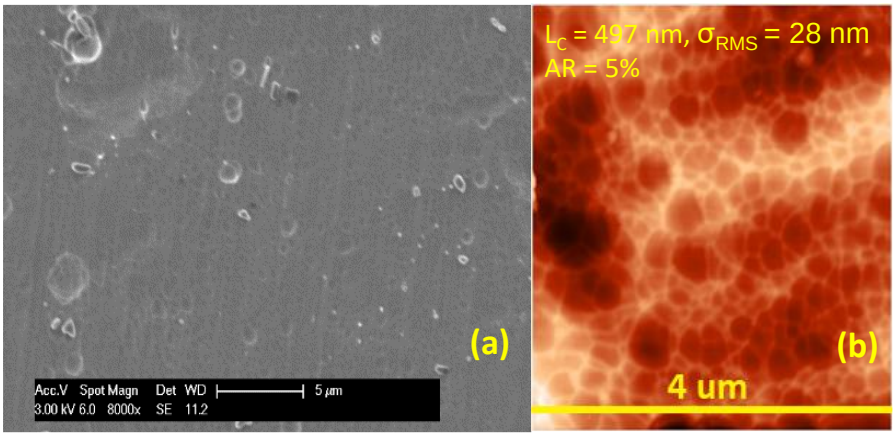

Figure 1.1. (a) SEM and (b) AFM images of the factory baseline textured Al foil.

It is clear from the SEM picture in figure 1.1 (a) that no micro-craters are found on the surface of the sample. Looking at the AFM in figure 1.1 (b), the autocorrelation is only ~500 nm and the roughness is ~30 nm. The aspect ratio is ~5%. Therefore, this is not high enough to grow high quality nc-Si:H. Indeed, when we deposit nc-Si:H on this type of substrate, the absorber layer has many structural defects, as depicted in the cross-sectional SEM image in figure 1.2.

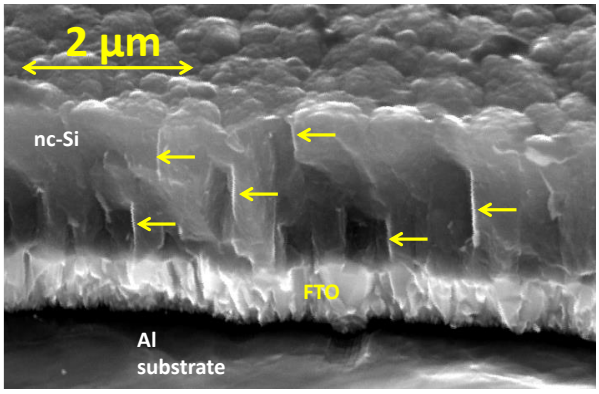

Figure 1.2 Cross-sectional SEM image of Al/TCO/p-i-n nc-Si:H. The yellow arrows correspond to structural defects inside the absorber layer.

The optical characterization of the factory baseline sample was also made. We measured the angular intensity distribution (AID) at λ = 800 nm. We also measured the total and diffused reflectance. The outcome is that this type of substrate is able to scatter mostly specular light and, across the whole spectrum, the diffused reflectance is really low (~30% on average). These results are highlighted in figure 1.3.

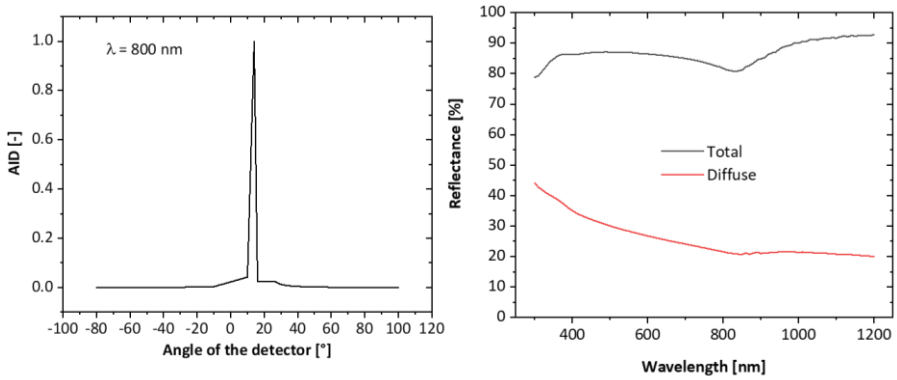

Figure 1.3 Optical characterization of the factory baseline Al substrate; (left) AID measured at λ = 800 nm, (right) total and diffuse reflectance across the whole solar spectrum.

Further, in order to give a direct metric of the optical characterization of the textured substrates, haze will be measured. It is referred to as the ratio between the diffused reflectance and total reflectance.

c. Alternative textured Al substrates

Subsequently, we had to understand the etching kinetic of NaOH with Al foil. Therefore, we measured the etching rate of Al in NaOH diluted in water at different etching temperatures. This has been done to understand what the maximum etching rate is that we can allow to our process. Indeed, a technical constraint is the minimum thickness of the foil that should not be below 100 µm. If this is not occurring, then the roll-to-roll process will have mechanical issues of stability and therefore cannot be completed. Figure 1.4 shows the etching versus concentration at different temperature. As expected, the etching rate increases with time and NaOH concentration.

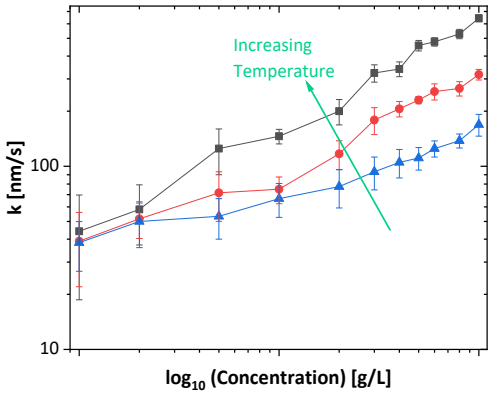

Figure 1.4 Etching rate versus NaOH concentration at different temperature.

With the thickness constraint in mind, we deliver better pre-treatment in reference to the baseline texturing. In order to be able to obtain good texturing, we have to move in a different regime. By employing the temperature-concentration chart as in figure 1.5, the bottom-left corner is the current industrial standard, also known as the factory baseline recipe, and we have to move towards to up-right corner to increase the etching rate to make larger craters.

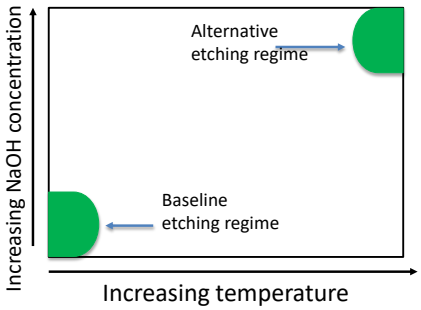

Figure 1.5 Temperature-concentration chart to justify our new textured Al substrates.

In the alternative etching regime we obtain structural properties shown in figure 1.6. Micro-craters are present on the surface of the aluminum foil. Correlation length and root-mean-square roughness are in the range of 3.8 µm and 480 nm, respectively. This gives an aspect ratio of ~12.5%.

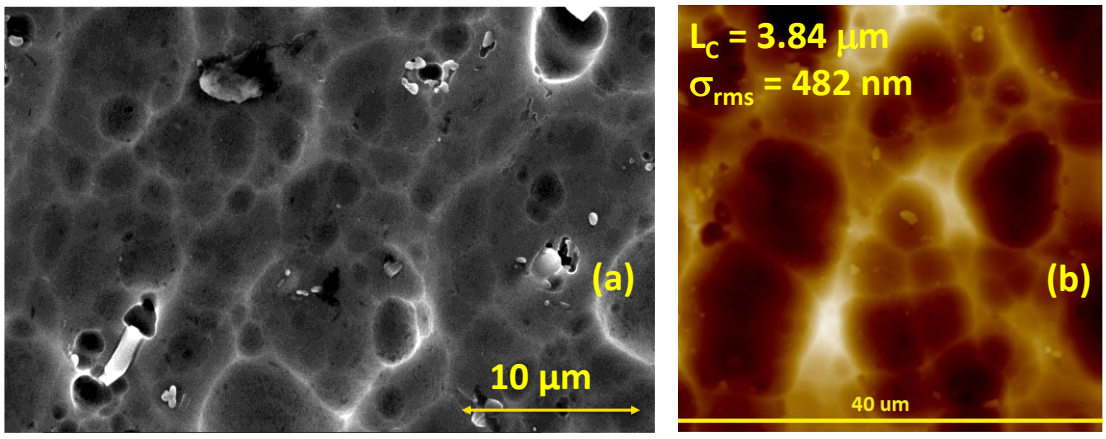

Figure 1.6 Improved textured Al substrate structural characterization, (a) top-view SEM, (b) AFM

An analysis of the etching time influence, keeping temperature and concentration constant, shows little influence on structural properties and aspect ratios. In figure 1.7, the etching time is varied from 2 to 3 minutes while temperature and concentration are still in the range of the top right figure in figure 1.5.

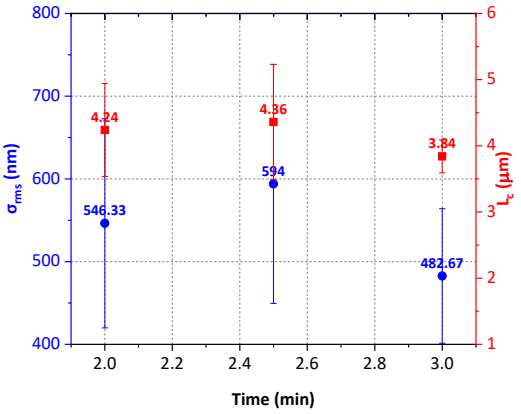

Figure 1.7 Correlation length and RMS roughness in the high temperature, high concentration regime at different etching times.

Therefore, the aspect ratio is in the range of 13%. This lab-scale sample is a good demonstrator for the high-quality substrate for tandem purpose. Indeed, when depositing a single junction nc-Si:H cell, a tandem or a triple junction a-Si:H/nc-Si:H/nc-Si:H solar cell, no visible cracks appear in the nc-Si:H absorber layer(s), as depicted in cross-sectional SEM images in figure 1.8.

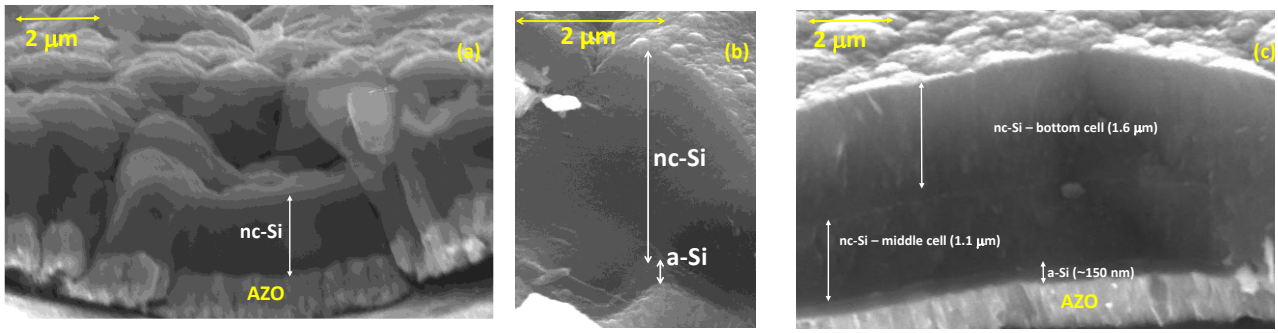

Figure 1.8 Cross-sectional SEM image of (a) nc-Si:H single junction, (b) a-Si:H/nc-Si:H tandem, (c) a-Si:H/nc-Si:H/nc-Si:H triple junction. No defects are shown in the nc-Si:H absorber layer.

Moreover, a single junction nc-Si:H solar cell (with AZO front window layer) has been completed with sputtered back contact. Then, it has been laminated and the temporary Al substrate has been etched. As shown in cross-section in Figure 1.9, the curved morphology has been correctly transferred to the laminated foil.

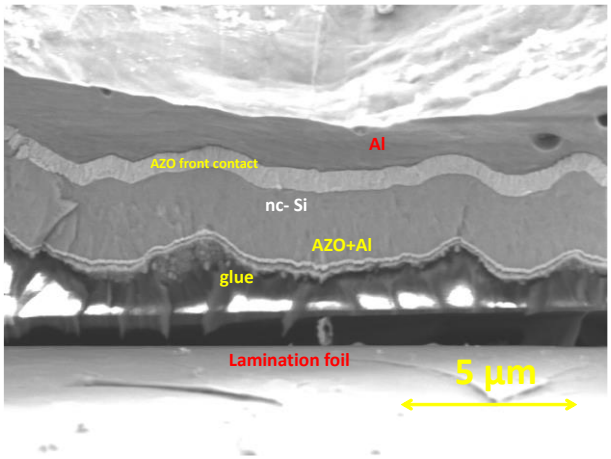

Figure 1.9 Cross-sectional SEM image of laminated nc-Si single junction device with nearly etched Al temporary foil.

d. Aluminum substrate pre-treatment: from lab to fab.

In order to be able to export the texturing foil from lab to fab-scale, we have to look at mechanical constraints of the roll-to-roll machines. As aforementioned, the foil thickness cannot go below 100 µm otherwise roll-to-roll process stability is lost. Therefore, we have to run specific experiments to understand what our process window can be to export the process to roll-to-roll. The initial aluminum foil thickness is 110 µm.

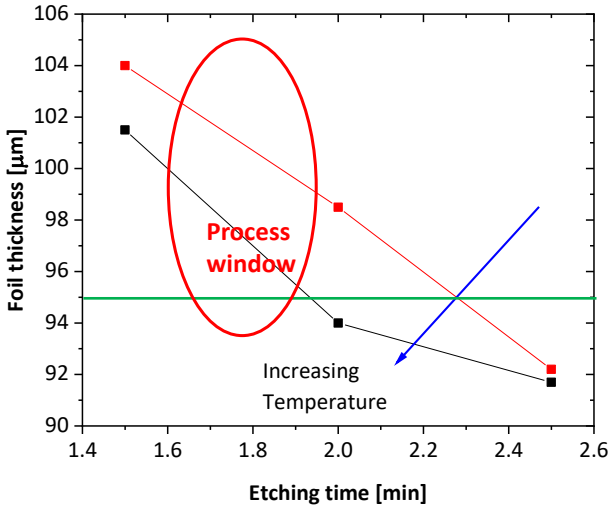

Figure 1.10 Correlation length and RMS roughness in the high temperature, high concentration regime at different etching times.

In figure 1.10, an etching time test (the dots in the figure) has been executed in order to understand an etching processing window for roll-to-roll demonstration. Keeping in mind the thickness constraint for roll-to-roll processing of 95 µm Al foil, a process window has been established for a roll-to-roll pre-treatment experiment. This roll-to-roll process has been named as FLAM01 and has been executed and characterized from a structural point of view. FLAM01 differs from the factory baseline recipe because it is in higher temperature etching regime. As shown in figure 1.11, micro-craters are appearing on the surface of Al substrate.

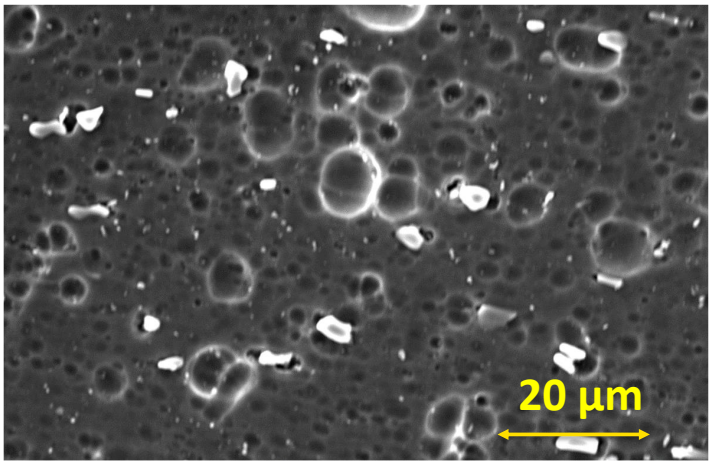

Figure 1.11 Top view of FLAM01-textured aluminum foil in roll-to-roll process.

As already noticed in the top-view SEM picture, the structures seem to be highly inhomogeneous. Indeed, large craters are alternated with smaller craters. To quantify this effect, we took AFM in two different positions on the foil (PoF) and calculated L_C and σ_{RMS}. As figure 1.12 shows, the foil is quite inhomogeneous at different PoFs.

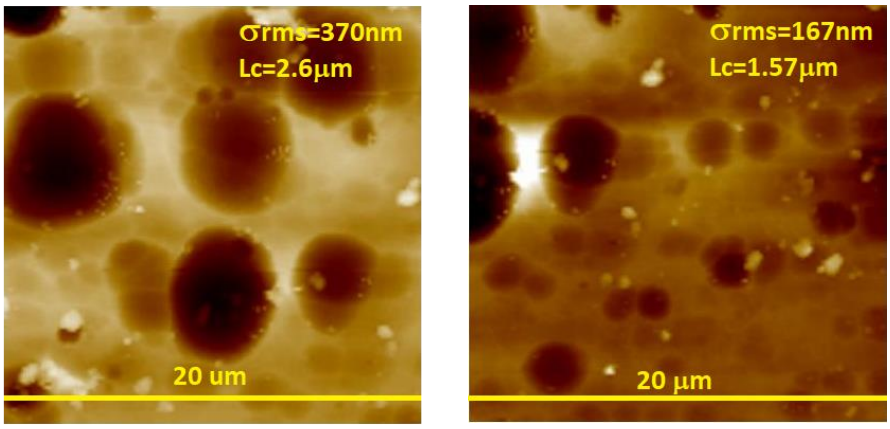

Figure 1.12 AFM measurements of FLAM01-textured Al substrate in different positions of the foil.

In a certain position of the foil, the L_C is 2.6 µm and σ_{RMS} is 370 nm (see figure 1.12 left), while in another position L_c is 1.57 µm and σ_{RMS} is 167 nm. However, the aspect ratio is in the range of ~ 11%. When we deposit a tandem device, we also observe very few cracks in the nc-Si:H absorber layer, as shown in figure 1.13. The two AFM images taken in two different spots show that the Al foil is still flat, despite having large craters as well as smaller craters. Therefore, the uniformity of the craters is also an important metric to take into account.

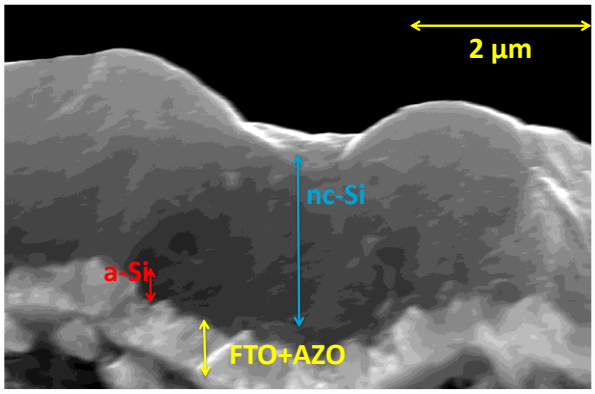

Figure 1.13 Cross-section of an a-Si:H/nc-Si:H tandem silicon layer stack deposited on FLAM01-textured substrate.

In order to replicate the lab-scale texturing in roll-to-roll configuration in a mechanically stable way, we have to deal with the foil thickness constraints. The replica, on the roll-to-roll scale, of the texturing developed in the laboratory at TUD is called FLAM02. The starting Al foil was 140 µm-thick, therefore the roll-to-roll process did not have any mechanical issues. In this way, the etched foil results in a thickness that is greater than 100 µm and the process can be mechanically safe.

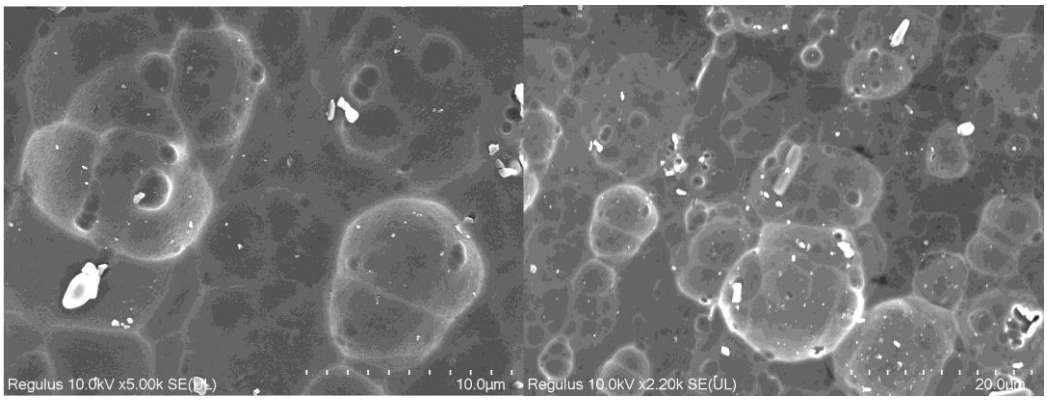

Figure 1.14 Top-view SEMs of FLAM02-textured substrate.

This pre-treated foil was characterized by confocal microscopy. In figure 1.15 (a), a picture of a FLAM02-textured sample under such a microscope is shown. It is clear that there are craters of micrometer size. By measuring the sharpness parameter S_{PC} in figure 1.15 (b), we find out that, among factory baseline produced in 2020 and in 2021, FLAM02 has the highest curvature of ~ 20000 1/mm, while the others are in the range of 5000 to 10000 1/mm. Note that having a high S_{PC} value can influence the quality of the deposited stack: higher values lead to sharper features, which can lead to more texture thus enhancing light trapping, but sharper features can also lead to more cracks that end up being shunts in the layer stack.

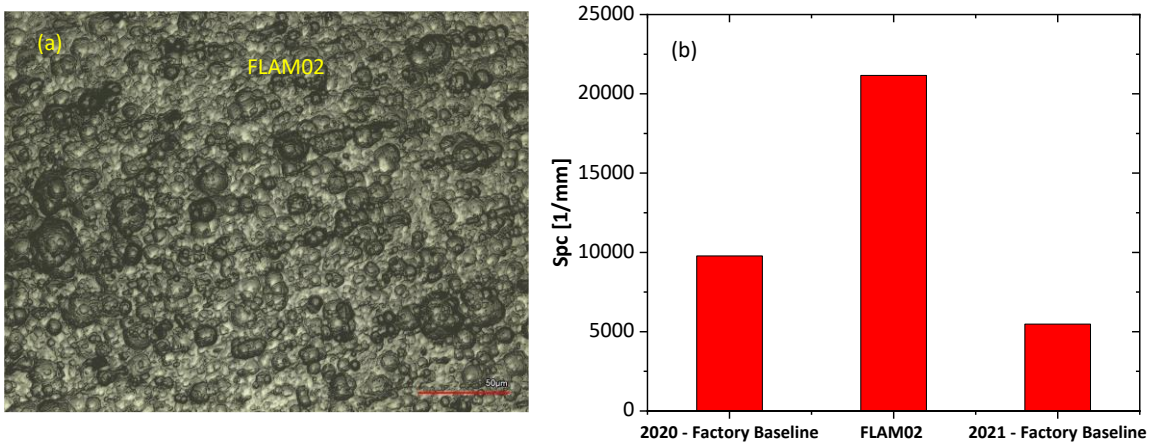

Figure 1.15 Top-view SEM of FLAM02 textured substrate.

e. Optical characterization comparison among different pre-treated samples

In this part, we measured optical properties of the pre-treated aluminum foils, factory baseline, FLAM01 and FLAM02. The first measurement is the angular intensity distribution at λ = 800 nm, as already shown in the factory baseline in figure 1.3. As displayed in figure 1.16, the scattering properties versus angle of incidence becomes more and more efficient when FLAM02 is deployed. Indeed, in this case, excellent scattering properties from -40 to 40 ° are found.

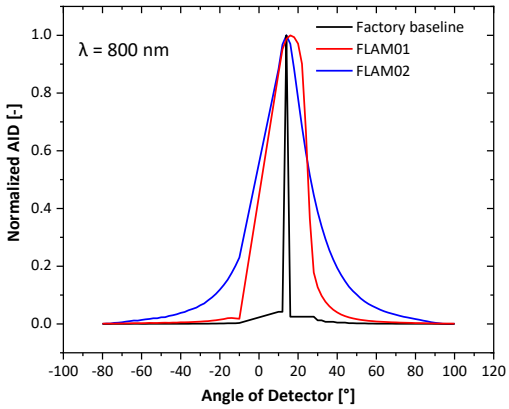

Figure 1.16 AID measurement of factory baseline, FLAM01 and FLAM02 textures.

Then, we measured the specular and diffuse components of the reflected light across the spectrum that is relevant for thin film multijunction solar cells and modules. In figure 1.17, the diffused reflectance is compared among the different pre-treated foils. It is clear that FLAM02 has the lowest specular reflectance and the highest diffused reflectance.

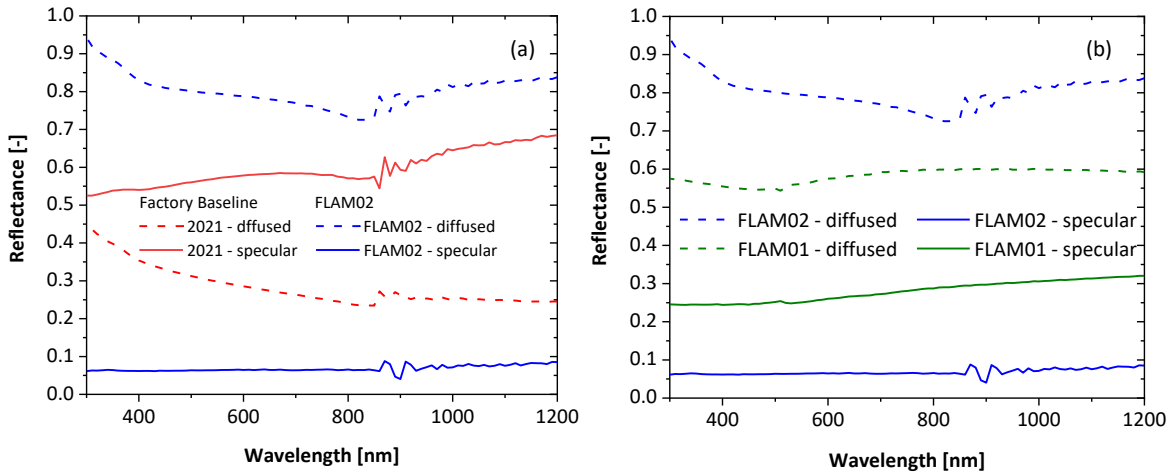

Figure 1.17 Diffused and specular reflectance measurement across the whole spectrum; (a) comparison between factory baseline and FLAM02, (b) comparison FLAM01 and FLAM02.

In order to give a unique metric for the quality of these pre-treated foils, we calculated the haze (as defined in section b.). Figure 1.18 shows the haze as a function of the wavelength.

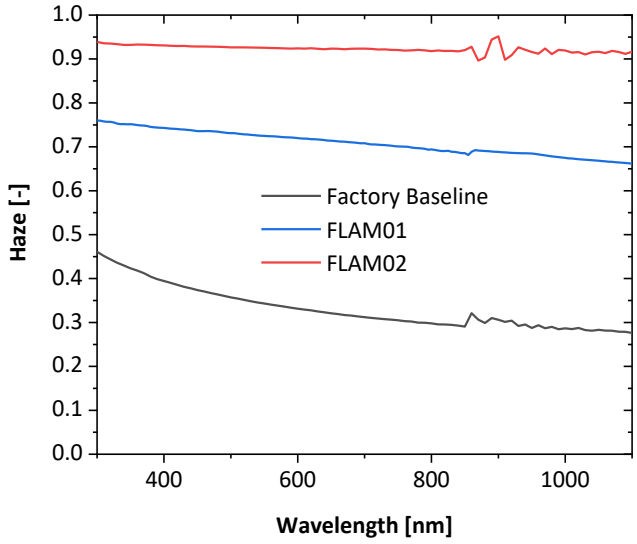

Figure 1.18 Haze calculation for factory baseline, FLAM01 and FLAM02.

It is clear how the haze is increasing from factory baseline to FLAM01 and FLAM02. Indeed, factory baseline has a haze between 30 and 50%, while the haze of FLAM01 is between 65 and 75% while the haze of FLAM02 is > 90% across the whole spectrum. This is important for tandem solar cell application as FLAM02 substrate will be able to scatter more light and therefore the absorption in the bottom cell will be increased.

f. Optical absorption simulation in solar cells for different pre-treatment.

To quantify the effect of the pre-treatment in the solar cell, we simulated the optical absorption with GENPRO4, an in-house software available at TU Delft. The simulated stack is depicted below in figure 1.19 (a) and the optical absorption in the top and bottom cell absorber layers are shown in figure 1.19 (b).

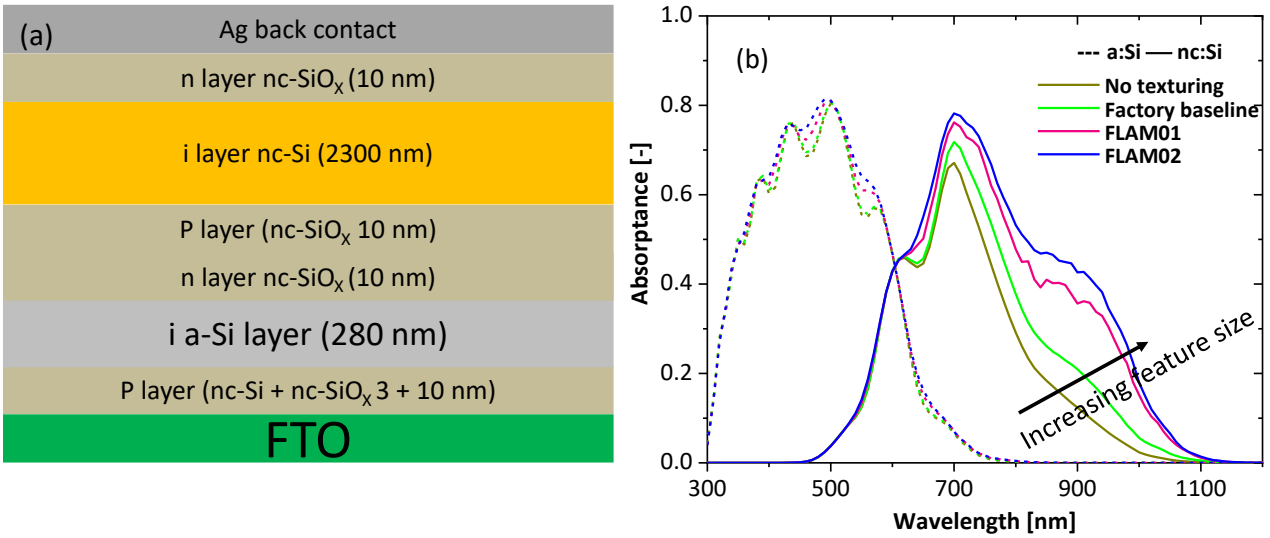

Figure 1.19 (a) Simulated stack with different pre-treatment in tandem solar cell application, (b) absorption in the top and bottom cell absorber layer at different pre-treatment.

The green curve represents the factory baseline, while the purple line is FLAM01 and the blue line is FLAM02. It is clear that increasing the feature size increases the absorption in the bottom cell, therefore facilitating high-efficiency design for a tandem solar cell. A quantification of such absorption is shown in the table below.

Texturing	Model	σ_{RMS} [nm]	Aspect ratio [%]	$J_{SC,\ top}$ [mA/cm^2]	$J_{SC,\ bottom}$ [mA/cm^2]
Factory baseline	Wave	28.4	5.7	10.05	9.88
FLAM01	Ray	233	10.26	10.1	11.45
FLAM02	Ray	594	13.58	10.12	14.36

Table 1 Simulated photogenerated currents in top and bottom cells in tandem configuration shown in figure 1.19 (a).

The bottom cell current is increasing from 9.8 to 14.3 mA/cm^2 from factory baseline to FLAM02 pre-treatment. The total spectral utilization is increasing from ~20 to 24.5 mA/cm^2.

2. Removal of precipitants from Al foil

From the SEM analysis done for TCO+Al based samples, we could observe the presence of white particle like structures scattered around the different areas of the aluminum substrate for the pre-treated samples as indicated below in figure 2.1a. However, these particles do not appear for the untreated samples, as shown in figure 2.1b. These particles are referred as the precipitants. The presence of these precipitants was observed for all the pre-treatment processes used which include factory baseline (FB), FLAM01 and FLAM02. Overall, the pre-treated samples appeared to have higher surface roughness which is believed to be caused due to these precipitants as indicated in figure 2.2, as well as the widening of the holes and sharpening of the foil morphology.

Fig 2.1a: Precipitants present in TCO+Al sample

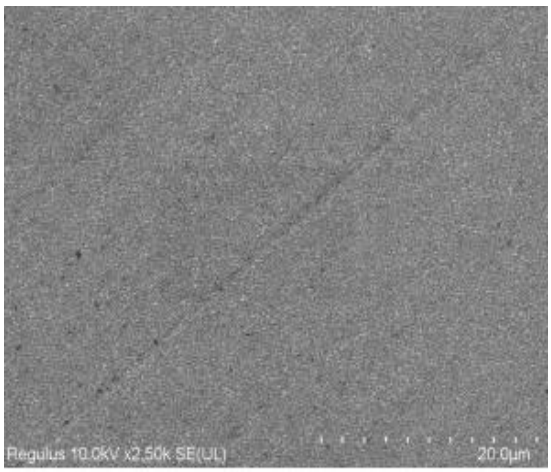

Fig 2.1b: No precipitants present in untreated TCO+Al sample

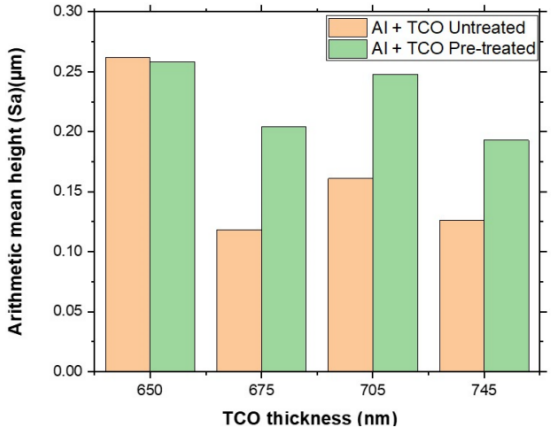

(a) Aritmetic Mean height(S_a) measurements

Fig 2.2: Surface roughness comparison

Despite these observations, the pre-treatment is necessary for texturing the foil to enhance light coupling into the cells which will enable generation of higher photocurrents thereby overall improving the efficiency of the solar modules. Previous experiments and simulations at HyET Solar demonstrate that the desired efficiencies greater than 12% on a tandem device cannot be achieved without pre-treatment. Also, the presence of pinholes, which seem to have a similar size and distribution as the precipitants, is found on the active area after etching which could hinder the current potential of the HyET modules. These precipitants could also have a negative impact on the morphology, optical, and electrical properties of the PV modules thereby ensuring lower performance. Therefore, in order to reach the desired efficiencies at HyET, it is essential to eliminate or greatly reduce their number in order to ensure a homogeneous surface for the depositions of the TCO and silicon layers. Their homogeneous deposition could overall lead to better performance gains.

Overall, the precipitants could be removed by either aluminum stretching or acid treatment. Among these processes, the acid treatment has been found to be the most reliable process towards removal of these precipitants which could also be replicated on production scale. This acid treatment is usually performed post the pre-treatment process with NaOH solution. EDX analysis has been carried out to determine the composition of the precipitants which will help determine the best approach to eliminate them.

From the EDX analysis, the composition of the precipitants was mainly found to Fe (concentration 9.75 +/- 7.27 %) followed by Mn (concentration 5.98 +/- 2 %) and Si (concentration 4.53 +/- 2.53%) and the size of the precipitants on average varies from less than 1 µm to a maximum of around 5-6 µm. In HyET Solar, the aluminum foil used for the production process is not 100% pure and usually a small quantity of elements such as iron, manganese and silicon are doped in it to boost its mechanical properties. This doping process is essential for the Al foil to be stable during the TCO as well as the silicon depositions. Therefore, these elements are what constitute the precipitants and it appears that the pre-treatment process exposes these precipitants when the aluminum etching takes place.

From literature, it was found that ultrasonication was the best method for removing particles especially in micron sizes. Different acids such as H_2SO_4, HCl, HNO_3, H_3PO_4 and PES acid etchant were tried for precipitant removal. Additionally, the samples were dipped in acid baths with and without ultrasonication for a time period ranging from 10 seconds to 5 minutes. The ultrasonicated acid baths showed promising results as they helped in removal of the precipitants. Overall, samples dipped in both PES and H_3PO_4 ultrasonicated acid baths were found to have much fewer precipitants at time intervals of 3 and 5 min, but the precipitants appeared to be replaced by holes as shown below by the SEM images in figures 2.3 and 2.4.

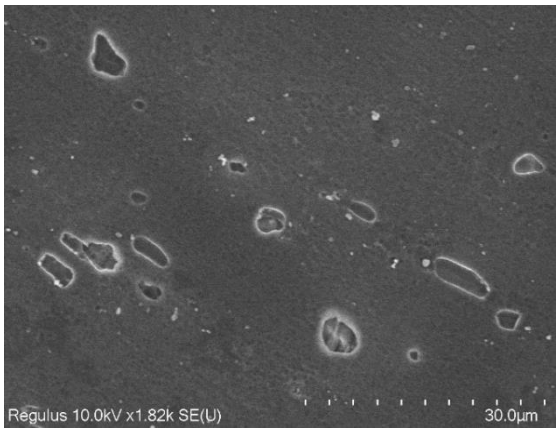

Fig 2.3: 5% H_3PO_4, 3 min dip, ultrasonicated

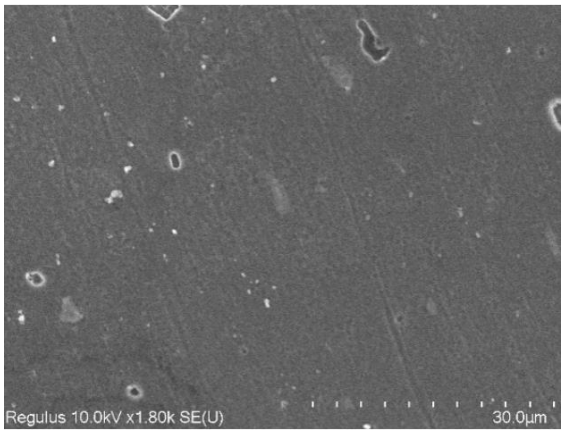

Fig 2.4: PES etchant, 3 min dip, ultrasonicated

Overall, from these set of experiments, it can be concluded that ultrasonication process in acid baths currently appears to be the best method to tackle the issues of the precipitants which are currently present in the aluminum foil at HyET. However, the best treatment for ensuring the overall improvement of PV performance is yet to be determined. Therefore, once the lab scale APCVD tool is commissioned, devices can then be made at lab-scale with and without the ultrasonic acid treatment to study the impact of the precipitants on the overall cell performance. Additionally, it is worth mentioning that the holes that replace the precipitants could also be problematic for film quality. Eventually it may be necessary to opt for a partial removal of the precipitants and look into the possibility of using foils with a smaller precipitant size and distribution.

3. Improving the quality of the interconnect in a module

The process through which the interconnections between neighboring cells are formed has been one of the main sources for performance losses, thus impacting efficiency, throughput, and yield. It consists of two laser scribes – P1s and P2s, where the P2s is responsible for current conduction across the module, and two ink lines – P1f and P3f, which are crucial to the process.

In 2021, there was evidence collected on how a bad interconnect would look like based on an optical inspection system, but the consistency could not be quantified. Upon performing SEM imaging at TU Delft on baseline scribes made by our

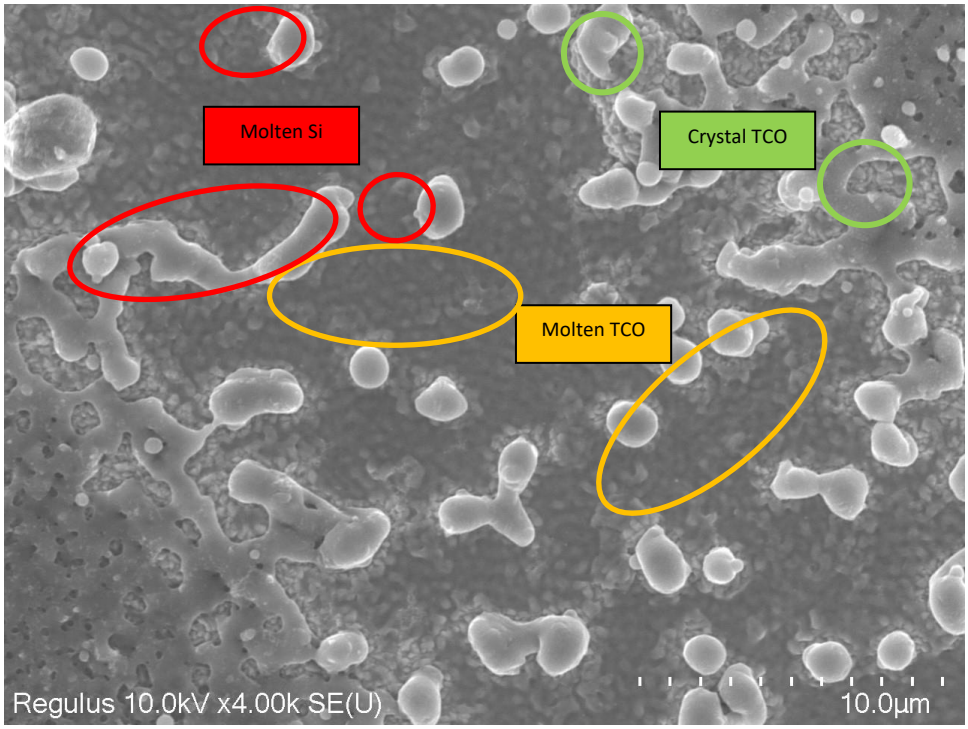

Figure 3.1 Baseline P2s scribe made with the old Spectra Physics lasers on the LP3 - October 2021

production machine on single junction material, it was evident that the P2s was open, but had completely molten TCO and had traces of molten Si on the conductive path (which one would expect to be a clear path of TCO crystals). This was attributed to the limitations of the hardware.

The laser setup utilized a singular laser module with an optical pathway that would split the beam into two individual beams to scribe the P1s and P2s tracks of the interconnect. This however had proved to be insufficient as the laser power of the P2s (the track responsible for the conduction across cells) was insufficiently open. Earlier this year, it was decided to upgrade the laser module of the production machine to regain good performance. To facilitate this upgrade, Solliance allowed us to perform tests on their IPG lasers to allow us to find an optimal laser setting on our material and the resulting scribes were analyzed under the SEM at TU Delft. This laser provided us with scribes with a conductive path that was wide enough and clear of any molten Si over the TCO.

There are two parameters that can be manipulated during laser scribing process; i) pulse energy and ii) frequency. The quality of the two scribes has a complex interplay between these two parameters. However, a general trend can be summarized by the idea that, with increasing pulse frequency, the energy pulse has to be lower to achieved the same scribing depth, as shown in figure 3.2. When the pulse frequency is reduced, then the energy pulse has to be increased in order to achieve deeper scribes. The reason for such a trend is due to the energy that is transferred to the substrate during the ablation process. For the P2s, it is quite critical that the scribe stops at the level of crystalline TCO, therefore, a space of parameters of energy and frequency pulse is studied. The frequency is swept between 10 and 33 kHz while the energy is swept between 1.1 and 4 µJ/pulse.

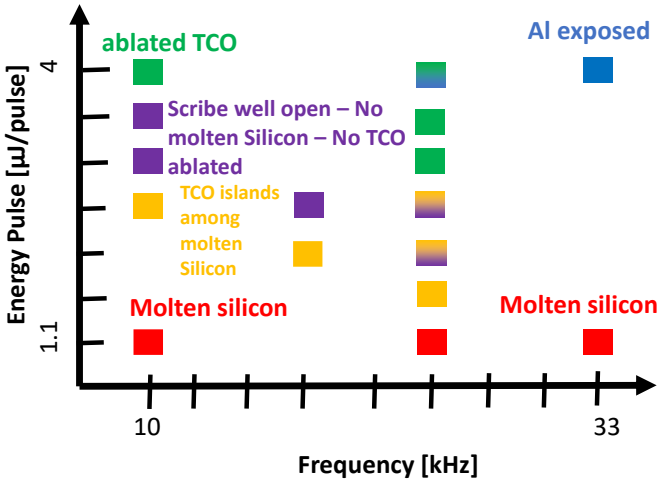

Fig 3.2 Trend of the laser scribe quality in the frequency – energy parameters of space based on SEM images.

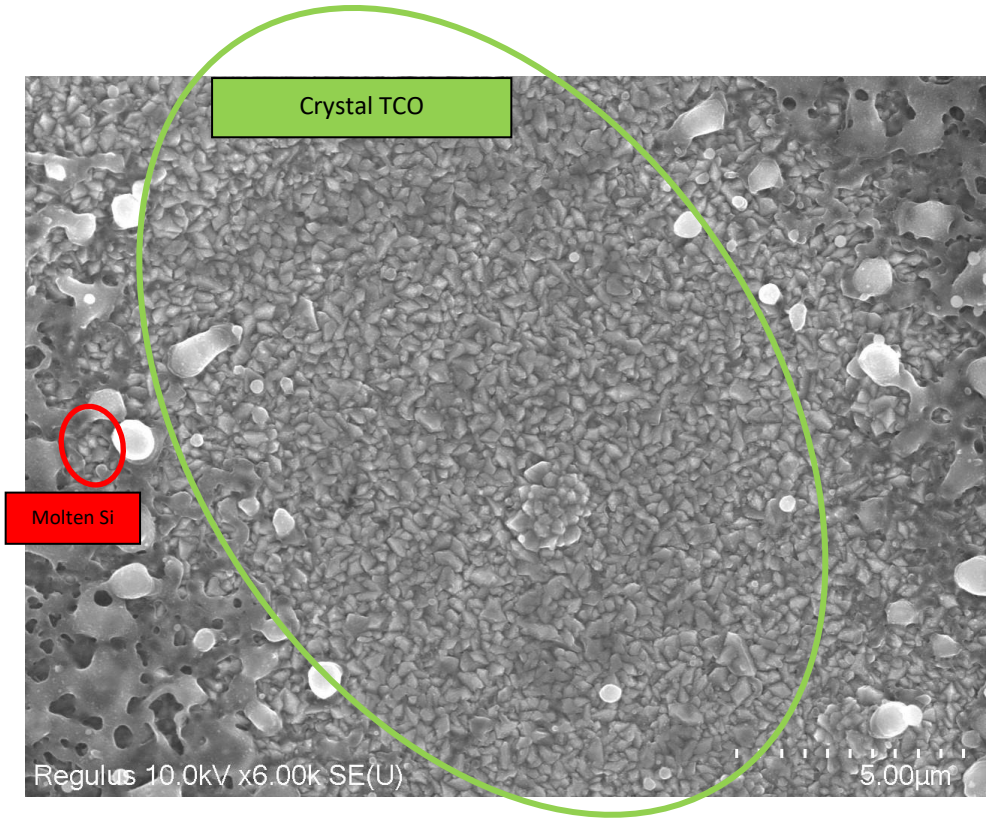

Figure 3.3 P2s scribes made with the IPG laser at Solliance at the process speed of the LP3 on single junction material. Pure TCO tracks were achieved.

In the image of the P2s above, the crystals of the TCO have been preserved well during ablation, while also ensuring that the Si is completely molten away from the track. This is the quality of the P2s scribe that has been sought out for. The IPG2LP3 project of implementing the new lasers and their optics was begun in Feb 2022 and it involved the procurement of two IPG GLPM-10 lasers, one for the P1s and the other for the P2s independently, and the first experimental results out of the lasers was released in June 2022. Over a few extra runs of finetuning and understanding new performance metrics, a quality algorithm was implemented that would allow for live monitoring of the P2s's quality while also ensuring the process is kept under control with a tweakable parameter.

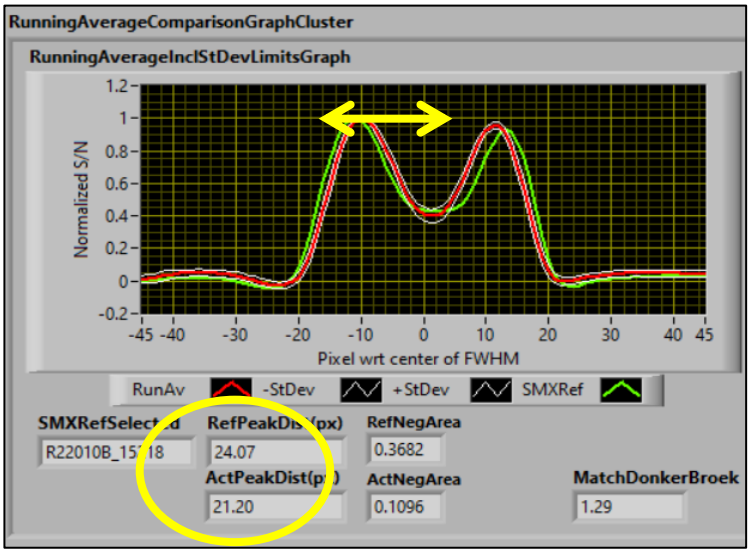

Figure 3.4 The new in-line quality diagnostics system. The optical data can now be visualized live with the reference data of the record performing module.

The green curve is the Reference from the best performing module of 2022, with a 7.81% efficiency and a 10.9 Ω-cm^2 R_{oc}. The red curve is a live average of the module being scribed on the machine. The qualifying parameter is the Peak distances. If the peak is lower than the reference, the laser power can be increased until they overlap, and vice versa. The idea is to keep the peak distances as close as possible by tweaking the P2s laser power.

4. Roadmap to reach 12% stabilized efficiency for tandem modules

To reach higher efficiencies a roadmap was devised to achieve 12% stabilized efficiencies of the roll-to-roll production of tandem modules. Here the initial efficiency for a top cell (ToC) and bottom cell (BoC) thickness of 300 nm and 1600 nm respectively was 8.3% which was achieved in the roll-to-roll production process. The collaboration with TU Delft played an important role in realizing this roadmap. The research output from the university is used as a starting point for the optimization of the roll-to-roll equipment. This results in reduced time and effort to find the optimum settings while enabling higher efficiencies within reach.

In the collaborative work between HyET Solar and TU Delft, there is a constant exchange of ideas, recipes, and samples. The high efficiencies achieved on glass samples are used as a starting point for making recipes on aluminum foil. These recipes providing high efficiencies are then translated to the roll-to-roll production process to make industrial-scale solar modules. The objectives shown in Table 4.1 is inspired by the research work performed already in TU Delft, demonstrating the high-efficiency building blocks.

S.No	Objective	Relative Efficiency increase (%)	Efficiency (%)	Source
	ToC 300 nm, BoC 1600 nm	N/A	8.3	Internal literature [7]
1	ToC 300 nm, BoC 2000 nm	7.2	8.9	Internal literature [7]
2	Dead zone from 650 micron to 350 micron	3.3	9.19	Internal literature [7]
3	ZAZAl back contact	11	10.21	Internal literature [7]
4	Encapsulation	3.5	10.56	Internal literature [7]
5	Modulated surface texture (FLAM01)	11.6	11.79	H Tan et al [3]
6	Optimize ToC p-layer	5.4	12.42	H Tan et al [8]

7	Optimize IRL in TRJ to redistribute current	1.6	12.62	M. Boccard et al [9]
8	Optimize BoC n-layer	5	13.25	S. W. Liang et al [10]
9	Optimize TCO nucleation: overall light absorption	1.5	13.45	Internal literature [7]
10	Stabilization SWE -10%	-10	12.11	Internal literature [7]

Table 4.1 – Illustrating the roadmap steps to achieve 12% stabilized efficiencies

The objectives are further characterized by different production processes. Objectives 1,6,7,8 involve optimization in the PECVD deposition process. The interconnect/back contact optimization involves objectives 2,3. Furthermore, objectives 4,5,9 involve post-lab/TCO/Texturing.

Objective 1 – ToC 300nm, BoC 2000 nm[7]

As seen from Figure 4.1 the simulation results based on GenPro4 (optical simulation tool created by TU Delft), an increased BoC thickness results in light absorption in the longer wavelength part of the light spectrum. This results in a more current generation for the device. In 2021 we deposited a tandem roll-to-roll with a ToC of 300 nm and BoC of 1600 nm. This resulted in an average J_{sc} (short-circuit current) of 8.65 mA/cm^2. This was further optimized in 2022 where a tandem device with a 2000 nm BoC was deposited again in the same roll-to-roll conditions. Here, the J_{sc} achieved was 9.33 mA/cm^2 resulting in about 7.9% relative gain in the current increasing efficiency.

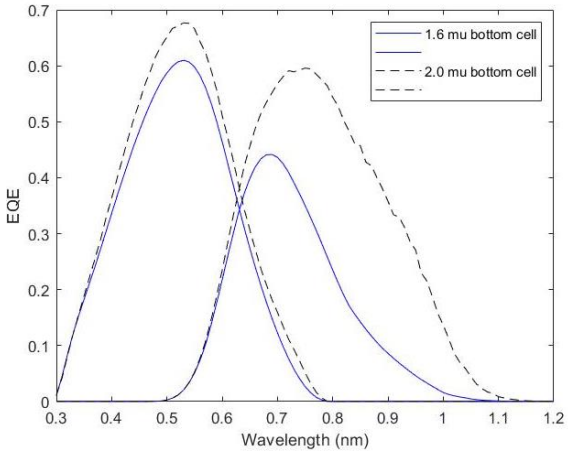

Figure 4.1 – Simulated EQE with varying BoC thickness [7]

Objective 2 – Dead zone from 650 micron to 350 micron[7]

The dead zone which is not part of the active area of the device reduces the light-absorbing part of the device. Hence, the goal is to reduce the current dead zone from 650 to 350 microns which can help us gain another 3.3% relative efficiency. The results shown in Figure 4.2 are simulated based on an ideal device with a sheet resistance (R_{sq}) of 14 Ω/sq where the effect of the dead zone can be understood. Furthermore, efforts are underway to demonstrate this effect on actual devices.

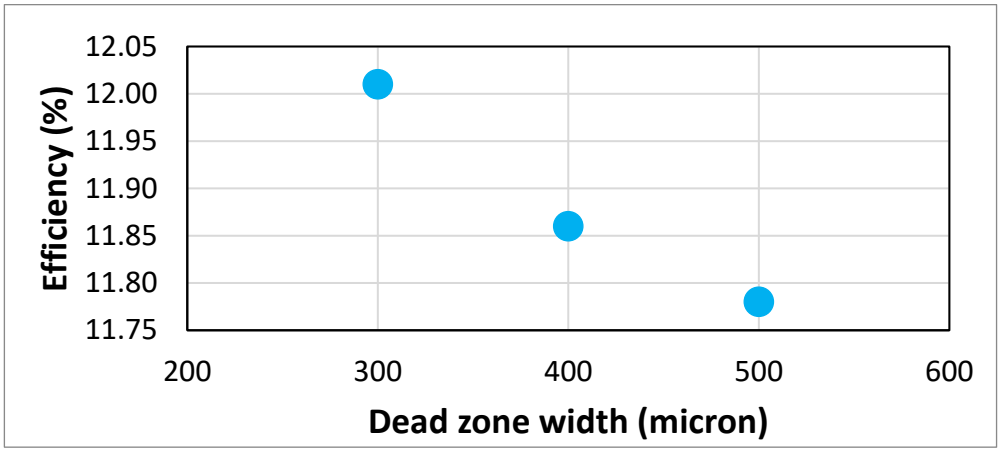

Figure 4.2 – Dead zone width as a function of the efficiency[7]

Objective 3 – ZAZAl back contact[7]

To increase the absorption by reflecting more light back into the device, a zinc oxide / silver / zinc oxide / aluminum (ZAZAl) back contact was implemented in 2022. This back contact comprises of silver which is more reflective than the traditional aluminum reflector. In Figure 4.3 the effect of ZAZAl back contact on the improvement of J_{sc} can be seen. Here the current gain is around 1 mA/cm^2, which can improve the efficiency by 11% relatively.

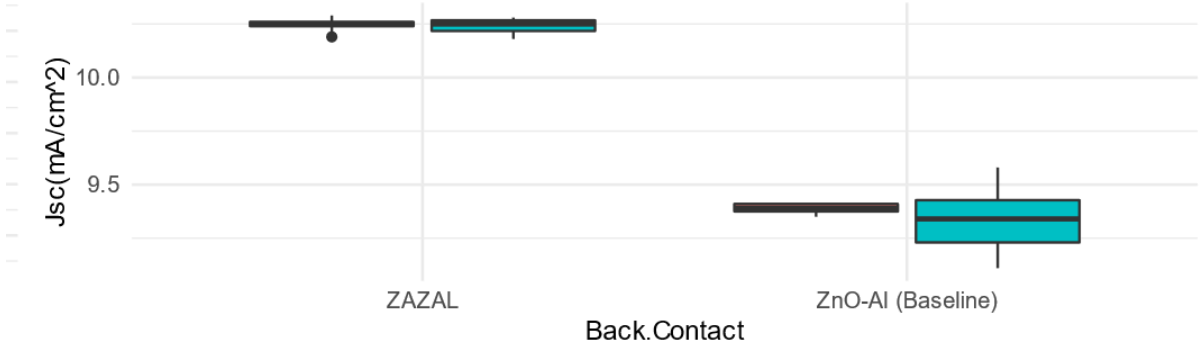

Figure 4.3 – ZAZAl vs. baseline ZnO/Al back contact effect on the J_{sc}[7]

Objective 4 – Encapsulation[7]

The tandem modules can be encapsulated which can enhance the current generation by enabling more light trapping in the device. The encapsulating layer further helps improve the reliability of the tandem modules as it protects against harsh weather conditions. In Figure 4.4 the positive effect of encapsulation on the J_{sc} can be seen where due to better light trapping the current generated by the device is boosted. The observed relative gain in efficiency after encapsulation is 3.5%.

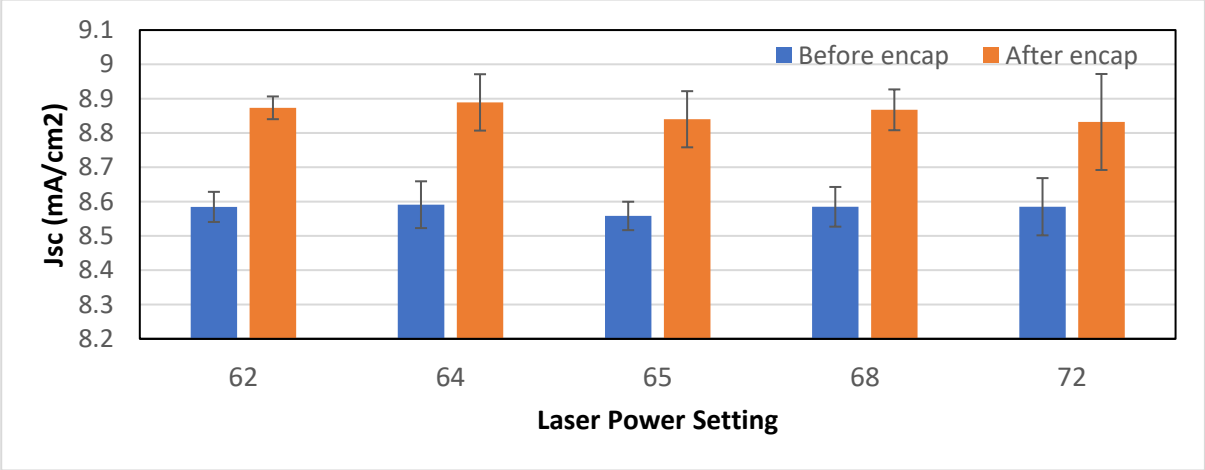

Figure 4.4 –Effect of encapsulation on J_{sc} (mA/cm^2) for different laser power settings[7]

Objective 5 – Modulated surface texture (FLAM01)[3]

The FLAM01 texture on foil, inspired on the modulated surface texture (MST) on glass, was developed in collaboration with TU Delft, where the current generated in both the top and the bottom cell of the tandem device is enhanced. This involves texturing to develop large and smooth features which are small and sharp as well as seen in Figure 4.5. The smooth large features promote the bottom cell growth while the small sharp features can help in enhancing the top cell current. It is expected that with the implementation of the FLAM01 texture, an 11.6% relative gain in efficiency can be achieved. Initial efforts have been made to mimic such a texture in the HyET Solar roll-to-roll production process.

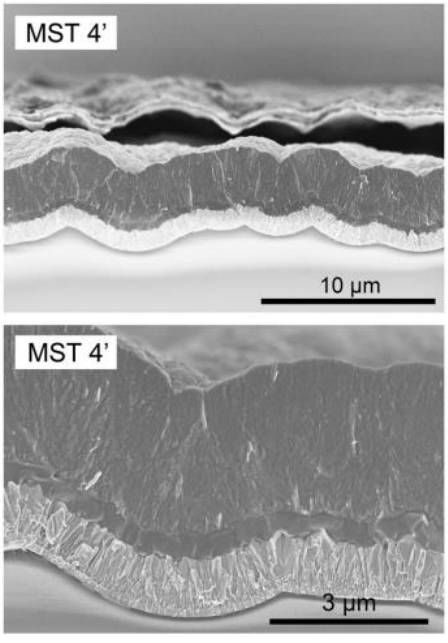

Figure 4.5 – High resolution cross section of tandem device on glass showing the MST with smooth and large features[3]

Objective 6 – Optimize ToC p-layer[8]

The p-layer in the ToC can play a critical role in boosting the open circuit voltage (V_{oc}) of the tandem modules. The double p-layer structure as researched by TU Delft involves having a thin p-type SiO_x layer with high doping levels acting as a contact layer and a thicker more transparent p-type SiO_x acting as the window layer. This structure ensures better holes collection at the front TCO enhancing the V_{oc} while the oxide layers ensure less parasitic absorption. The p-layer optimization was carried out in the roll-to-roll production process where the highest V_{oc} achieved was 0.918 V which is a 0.030 V increase from the baseline single junction devices. The optimization was carried out in the PECVD tool using the state-of-art automatic recipe generating tool where numerous settings were investigated to achieve higher V_{oc}. The expected relative increase in the efficiency for such a double layer was 5.4% [8].

Objective 7 – Optimize IRL in TRJ to redistribute current[9]

The intermediate reflection layer (IRL) in the tunnel recombination junction (TRJ) serves the purpose of distributing the light in both ToC and BoC. The ToC can gain in current by ensuring that the low wavelength light is reflected in the top absorber while the bottom absorber can receive the higher wavelength spectrum of incoming and reflected light. The p-layer in the TRJ was optimized in 2022 tandem roll-to-roll production run where various settings based on different doping and deposition conditions were investigated. The optimum thickness of TRJ with the optimized refractive index properties can help improve the efficiency by 1.6% in relative terms.

Objective 8 - Optimize BoC n-layer[10]

The bottom cell n-layer can be deposited as a SiO_x layer which can reduce the parasitic absorption in the layer making it more transparent. Hence, when coupled with the ZAZAl back contact, the efficiency can improve 5% relatively. This effect has been demonstrated on lab-scale devices and amorphous single junction modules. However, for the bottom cell this is still to be investigated.

Objective 9 - Optimize TCO nucleation[7]

The TCO acts as a front layer for the light to enter the solar device. The current TCO used is FTO (fluorine-doped tin oxide) which is deposited using the roll-to-roll APCVD process. The nucleation layer plays an important role in influencing the mobility of the charge carriers, while the bulk TCO layers influence the overall absorption of the TCO. Hence, efforts are to be made to improve the sheet resistance of the TCO and make less absorbing FTO layers. The LAC (Lab-scale APCVD Coater) is going to be instrumental in developing a better FTO layer for tandem modules. The expected increase in efficiency is 1.5% relatively.

Objective 10 – Stabilization (SWE)[7]

The Staebler-Wronski effect (SWE) is a notorious behavior of amorphous silicon-based solar devices where due to light-induced degradation the efficiencies are reduced after prolonged light exposure. Based on our roll-to-roll production tandem modules we expect a relative decrease of 10% in efficiency after 168 hours of light exposure, as seen in Figure 4.6. This is considered when designing this roadmap to make a more industrial-ready product. Hence, in our roll-to-roll production process, the optimizations will be carried out for reduced ToC thickness to lessen the effects of light-induced degradation.

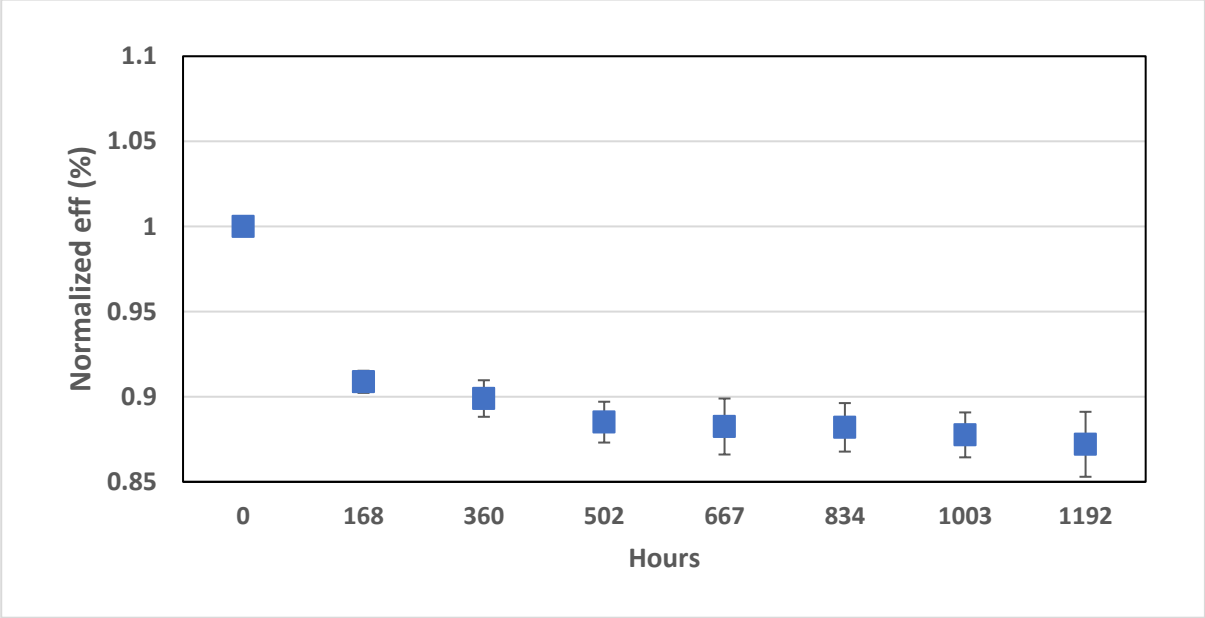

Figure 4.6 – Staebler-Wronski effect seen on our tandem modules reducing efficiencies after exposure to light

5. Life cycle assessment analysis

Life-cycle assessment of thin-film, lightweight, silicon-based solar panels has been carried out in this project. In this work, we defined our functional unit as a PV system made by HyET Solar technology with a rated power of 2.1 kW_p. The system is installed in Arnhem, The Netherlands, facing south at an inclination angle of 30°. The analysis type is cradle-to-gate and the boundaries are that transportation/maintenance is not included and no pass/fail results are given. Moreover, utilization losses real-time data from HyET Solar is used. Three scenarios are considered: i) a-Si:H single junction module with 7% efficiency, ii) a-Si:H/nc-Si:H tandem module with 10% efficiency (conservative case), and iii) a-Si:H/nc-Si:H tandem module with 12% efficiency. The life cycle inventory analysis has been carried out in collaboration with HyET Solar and it is shown below.

Process step	Material implemented
Pre-treatment	Aluminum, chemicals
Silicon	Silane Hydrogen - Dopants
TCO	Oxide-based materials
Encapsulant	Plastic material + Glue
Al substrate	Aluminum 99% grade
Heat/Electricity	Natural gas Heat/Medium-voltage electricity from NL
Inverter	Electronic component

Table 5.1 Life cycle Inventory analysis for HyET Solar

The main metrics to evaluate the environmental performance are i) global warming potential (GWP) and ii) energy payback time (EBPT). The first is measured in kg CO_2-equivalent. It represents greenhouse gas emission associated with the product manufacturing/use. EPBT represents the amount of time that the PV system has to operate to recover from the initial energy investment. It is typically measured in years. It is simply calculated as cumulative energy demand divided by energy produced in a year.

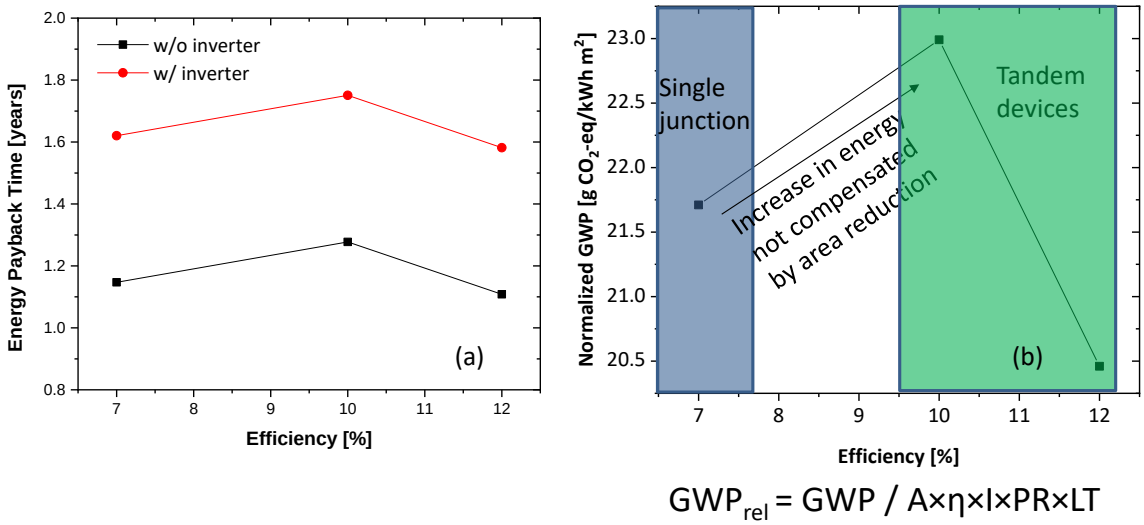

Figure 5.1 (a) EPBT versus efficiency (b) Relative GWP versus efficiency

The first calculation concerns the EPBT and GWP as a function of the efficiency of the modules, as shown in figure 5.1. The shift between the two curves in the EBPT figure represents the insertion of the inverter for the PV system. The inverter adds up to ~6 months to the payback time. For the trend, the worst case is 10% efficiency, because the tandem product requires more energy to be manufactured, but the increase in efficiency does not compensate the increase in energy. Also for GWP, displayed in figure 5.1 (b), the same trend is observed. The relative GWP is calculated taking into account the area, the performance ratio, the efficiency and the insolation constant and lifetime. Currently, the modules are 30 cm-wide.

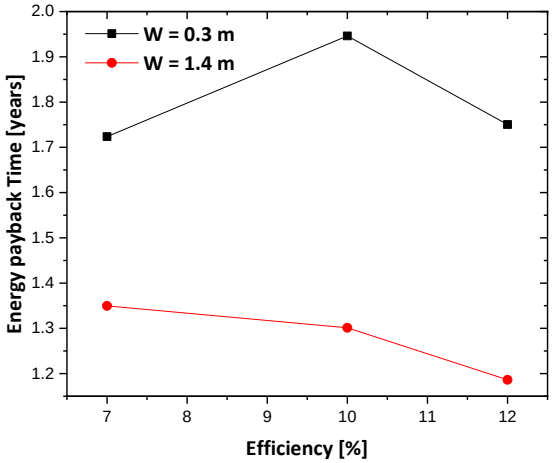

Figure 5.2 EPBT comparison between 30 and 140 cm-wide modules produced by HyET Solar.

In the short-term future, it is foreseen that the factory expands to 140 cm-wide modules. Therefore, the throughput is increased. In figure 5.2, the two cases of 30 and 140 cm-wide modules have been compared using EBPT. It is clear how the case of 140 cm is much more favorable from the EBPT point of view.

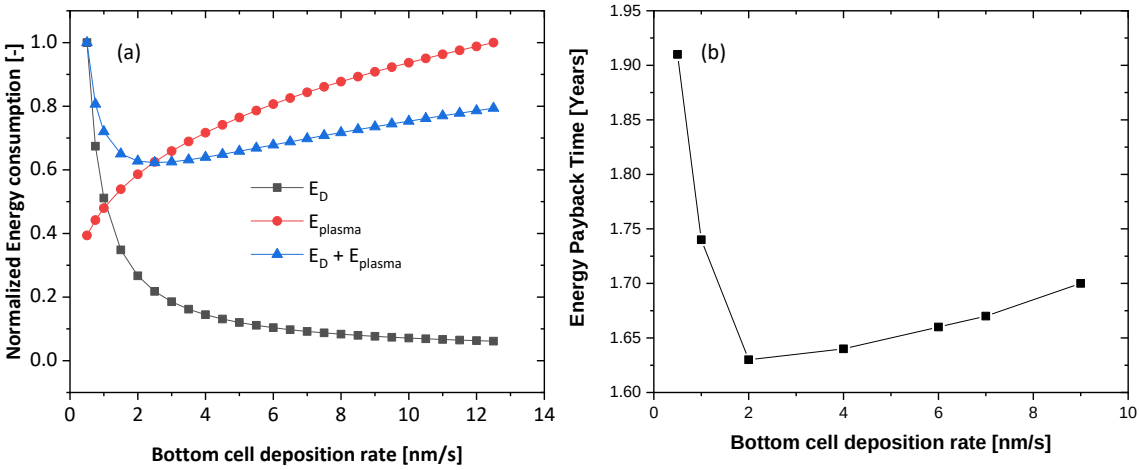

Figure 5.3 (a) Energy consumption of different PECVD components versus bottom cell deposition rate, (b) EBPT versus bottom cell deposition rate at 10% efficiency

The next analysis has been to look at bottom cell deposition rate. This is a critical parameter to increase the throughput of the factory in case of tandem solar module mass production. The focus is on different components of PECVD for the bottom cell production. Indeed, the higher the bottom cell deposition rate is, the higher the energy demand by the plasma becomes (E_{plasma}). At the same time, the increasing deposition rate requires less energy for the thermal management of the PECVD (E_D), therefore this component reduces its energy demand [6]. These results are summarized in figure 5.3 (a). The optimum to minimize the energy consumption is 2 nm/s. This is reflected in figure 5.3 (b), where the EPBT has a minimum at 2 nm/s.

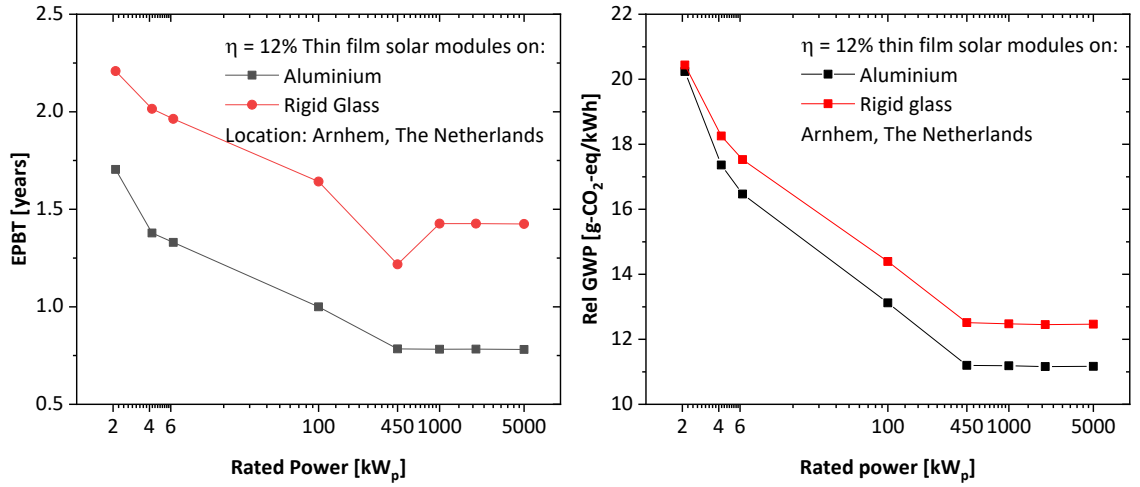

Figure 5.4 (a) EPBT versus rated power for rigid and flexible solar modules (b) relative GWP versus rated power for rigid and flexible solar modules

Subsequently, we investigated at large scale utilities and evaluated both EBPT and GWP and compared the flexible and rigid solar module technologies. Figure 5.4 displays the difference in performance when the location is Arnhem. It is clear that the flexible technology is outperforming the rigid solar cell technology. Both EPBT and GWP are lower when the rated power is increasing. Beyond 450 kW_p, the values are saturating because the increase in rated power does not compensate the area increase. Moving the analysis location to Perth, Australia, the situation is really similar, as shown in figure 5.5. The EBPT is much lower due to higher level of irradiation in Australia compared to The Netherlands. Still, from EBPT metric, the flexible technology outperforms the rigid one.

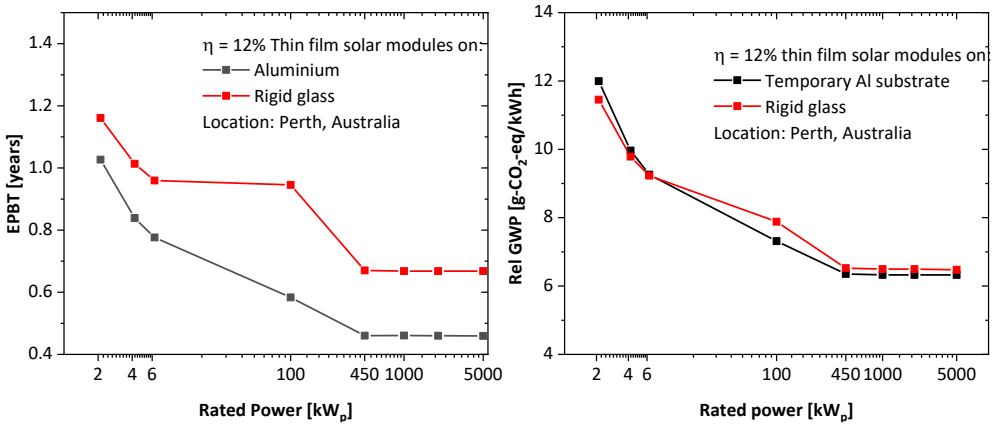

Figure 5.5 (a) EPBT versus rated power for rigid and flexible solar modules (b) relative GWP versus rated power for rigid and flexible solar modules in Perth, Australia.

Once again, beyond 450 kW_p, the trend saturates because the increase in energy production is balanced by a proportional increase in area and material consumption.

6. References

[1] H. Sai et. al., Appl. Phys. Lett 101, 173901 (2012).
[2] H. Tan et al, Appl Phys. Lett. 103, 173905 (2013).
[3] H. Tan et. al., Prog. Photovolt.: Res. Appl. 23, 949 (2015).
[4] T. Matsui et. al., Jpn. J. Appl. Phys. 54, 08KB10 (2015).
[5] H. Sai et. al., Appl. Phys. Lett. 102, 053509 (2013).
[6] E.A.G. Hamers et. al., Plasma Process. Polym. 4, 275 (2007).
[7] HyET Solar literature
[8] H. Tan et al., Sol. Energy Mater. Sol. Cells 132, 597 (2014).
[9] M. Boccard et al., IEEE J. Photovolt. 4, 1368 (2014).
[10] S. W. Liang et al., Jpn. J. Appl. Phys. 53, 05FV08 (2014).

Beschrijving van de bijdrage van het project aan de doelstellingen van de regeling (duurzame energiehuishouding, versterking van de kennispositie)

Programmalijn doelstellingen	Concrete (indien mogelijk kwantitatieve) bijdrage van het project aan de gestelde programmalijndoelstellingen
Het verlagen van de turnkey zonnestroomsysteemkosten met ten minste 20% in 2020 en ten minste 50% in 2030 (ten opzichte van de situatie in 2015) door het verhogen van het omzettingsrendement (watt-piek(W_p)/m^2) met ten minste 20% in 2020 en ten minste 35% in 2030 (ten opzichte van de situatie in 2015) en het verlagen van de fabricage- en installatiekosten van individuele componenten met ten minste 40% in 2025 (ten opzichte van de situatie in	The objective of FLAMINGOPV has been to increase the efficiency of the HyET flexible solar module from 10% to over 12%. When fully realized, this will reduce the production cost of the modules by 20%. The integration of the flexible lightweight modules allows for extremely low BoS costs. The further development of production tools and subsequent upscaling will drastically reduce the material costs based on existing quotes. The learning rate based on the rebates on material costs alone is 23%.

2015); deze kosten verschillen per toepassing.	
Het verhogen van de energieopbrengst van zonnestroomsystemen (kWh/W_p) onder praktijkcondities (dat wil zeggen van standaardcondities afwijkende lichtinstraling, temperatuur, spectrum, etcetera) tot ten minste 850 kWh/W_p in 2020 en 900 kWh/W_p in 2025 voor zonnestroomsystemen in Noord-West Europa, en door het toepassen van dubbelzijdig werkende (bifacial) panelen en diverse andere innovaties op module- en systeemniveau.	Although the SMART targets of this project are expressed in STC efficiency, the results of the project have allowed for an optimization of the module design (ratio thickness top versus bottom cell) for best energy yield in the various climates. HyET Solar in all their communications with clients always stresses the importance of LCOE as determining key performance indicator and not the STC efficiency.
Het verlagen van de kosten voor onderhoud en beheer, het langer behouden van een stabiele opbrengst tot ten minste 80% van het initiële energieopbrengst na 30 jaar in 2020 en 35 jaar in 2025, en het verlengen van de levensduur van PV-modules tot minimaal 30 jaar in 2023 en 40 jaar in 2030, inclusief methoden om dit (op een voor investeerders relevante wijze) te bepalen.	The HyET module is based on earth-abundant and non-toxic materials and uses moisture insensitive PV technology. The integrated manufacturing (all raw materials in, product out) in combination with very long-standing relations with the key material suppliers and the bilateral material developments with them have allowed to improve on module reliability. Fundamental insights into the materials as well as processing have made this progress possible. Sometimes reliability failed un-expectedly, forcing to find better and more severe accelerated lifetime tests and develop state-of-the-art quality assurance methods in production
Het verhogen van de esthetische kwaliteit door onder meer kleur- en textuurvariatie, (semi)transparantie, maat- en vormvrijheid.	The HyET Solar production sequence and product have several of these properties: the front sheet is slightly textured to reduce non-esthetical glance, modules in a range of colors are possible with commercially available colored durable polymers that are used in architectural appliances, the length of the modules is variable with 1 mm resolution, the end shape of the module can be user defined and aesthetical and functional coverage of available area. Prototypes of transparent PV modules have been made.
Het verbeteren van de veiligheid en de elektriciteitsopbrengst door het ontwikkelen en toepassen van innovatieve elektrotechnische systeemcomponenten o.a. voor het verhogen van de schaduwlineariteit.	The thin film technology with long narrow cells and monolithically integrated bypass diodes results in a high degree of shadow linearity in the single junction product of HyET Solar. This process needs to be fully tested and demonstrated in the tandem junction modules.
Het verbeteren van de integrale duurzaamheid van het complete systeem	Parallel to this project (not within the scope of FlamingoPV) the product has been in PV systems with special attention to the invertor specifications and closely monitored.

Rijksdienst voor Ondernemend Nederland

Spin off binnen en buiten de sector

Not applicable.

Overzicht van openbare publicaties over het project en waar deze te vinden of te verkrijgen zijn

(Overview of public publications about the project and where to find or obtain them)

1. Oral presentation, IEEE PVSC, 2022, Gianluca Limodio, S. Makhlouf, Edward Hamers, Arno Smets, Life Cycle Assessment analysis of thin-film, flexible solar panels produced in the Netherlands
2. Poster Presentation, WCPEC-8, 2022 G.Limodio, S. Makhlouf, V. Parameswaran, E. Hamers, A.H.M Smets, Life cycle assessment of thin-film, flexible, silicon-based solar modules: a techno-economic analysis.
3. Poster Presentation, AsianPVSEC 2022, G. Limodio et. Al., Life cycle assessment of thin-film, flexible, silicon-based solar modules: a techno-economic analysis.
4. Oral Presentation, AsianPVSEC 2022, G. Limodio et. Al., Modulated surface texturing of temporary Al foils substrates for high-efficiency thin-film, flexible solar cells.
5. Poster presentation, EUPVSEC, 2021, G.Limodio, D.Bartesaghi,G. Padmakumar, E. Hamers, A.H.M Smets, Modulated surface texturing of temporary Al foils substrates for high-efficiency thin-film, flexible solar cells.

Meer exemplaren van dit rapport

Meer exemplaren van dit rapport kunnen digitaal worden verkregen via het hieronder genoemde contact.

Contact voor meer informatie

Meer informatie over dit project kan verkregen worden via:

- de heer Edward Hamers, HyET Solar B.V., edward.hamers@hyetsolar.com
- de heer Arno Smets, TU Delft, a.h.m.smets@tudelft.nl

Subsidie

Dit project is uitgevoerd met subsidie van het Ministerie van Economische Zaken en Klimaat, subsidieregeling Top Sector Energie uitgevoerd door Rijksdienst voor Ondernemend Nederland.